

## Evidence for magnetoplasmon character of the cyclotron resonance response of a two-dimensional electron gas

C. Faugeras,<sup>1</sup> G. Martinez,<sup>1</sup> A. Riedel,<sup>2</sup> R. Hey,<sup>2</sup> K. J. Friedland,<sup>2</sup> and Yu. Bychkov<sup>1,3</sup>

<sup>1</sup>Grenoble High Magnetic Field Laboratory, CNRS, B.P. 166, 38042 Grenoble Cedex 9, France

<sup>2</sup>Paul Drude Institute, Hausvogteiplatz 5-7, D-10117 Berlin, Germany

<sup>3</sup>L. D. Landau Institute for Theoretical Physics, Academy of Sciences of Russia, 117940 Moscow V-334, Russia

(Received 28 June 2006; revised manuscript received 11 September 2006; published 24 January 2007)

Experimental results on the absolute magnetotransmission of a series of high density, high mobility GaAs quantum wells are compared with the predictions of a recent magnetoplasmon theory for values of the filling factor above 2. We show that the magnetoplasmon picture can explain the nonlinear features observed in the magnetic field evolution of the cyclotron resonance energies and of the absorption oscillator strength. This provides experimental evidence that inter-Landau level excitations probed by infrared spectroscopy need to be considered as many body excitations in terms of magnetoplasmons: This is especially true when interpreting the oscillator strengths of the cyclotron transitions.

DOI: [10.1103/PhysRevB.75.035334](https://doi.org/10.1103/PhysRevB.75.035334)

PACS number(s): 78.67.De, 78.20.Ci, 78.40.Fy

### I. INTRODUCTION

Many theoretical reports<sup>1-4</sup> have clearly stated that excitations between Landau levels (LL) of a two-dimensional electron gas (2DEG) subjected to a magnetic field  $B$  have to be analyzed, because of many body interactions, as excitonic transitions which are often referred to as magnetoplasmons (MP). These excitations display a specific dispersion as a function of the two-dimensional wave vector  $\vec{K}$  of the exciton. Because of Kohn's theorem<sup>5</sup> which states that no manifestations of electron-electron interactions can be observed in cyclotron resonance (CR) experiments unless the translational symmetry is broken or nonlocal potentials are present [giving rise to nonparabolicity (NP) effects, for instance], it was considered that the departure from the one-electron model due to the MP response should hardly be seen experimentally. However, when NP effects are present, the theory<sup>3,4</sup> predicts a mixing of the MP modes for small values of  $\vec{K}$  which could be, *a priori*, visible in experiments. Some signatures of coupled cyclotron resonance modes have already been observed in past years<sup>6,7</sup> but these works focused on low density samples and as a consequence on values of the filling factor below 2, a limit which is nowadays well understood in terms of coupled transitions in a two-component system, with a coupling even observed at high temperatures.<sup>7</sup> More recently, Manger *et al.*<sup>8</sup> studied the cyclotron resonance response of high density samples similar to the ones presented in this work and for integer values of the filling factor. The observed behavior in this case is different from the previous studies as the coupling disappears for a temperature higher than 1.4 K. These authors show that the one electron picture fails to interpret the oscillator strength of the split cyclotron resonance line. In a more recent report,<sup>9</sup> the conductivity of a 2DEG in the Faraday configuration (the light vector  $\vec{q}$  being parallel to the magnetic field  $\vec{B}$  and perpendicular to the plane of the 2DEG) has been calculated in the frame of the MP picture. We will present in this paper a detailed comparison of experimental results obtained in a quantitative way with the predictions of the MP model derived in the Hartree-Fock approximation ignoring

impurity and spin-orbit interactions for integer and noninteger values of the filling factor. We will show that the magnetoplasmon picture can explain some of the features observed in the cyclotron resonance response of a 2DEG.

A CR transition line is characterized by its energy position, its linewidth, and its intensity. Electron-electron interactions being nondissipative to first order, the MP should not contribute to the linewidth of the transition but both the energy position and the intensity of the CR transitions are expected to be modified. In the one-electron picture of CR, for noninteger values of the filling factor greater than 2, one expects three distinct transitions between successive Landau levels which conserve the spin. One of the predictions of the MP model<sup>9</sup> is that the excitonic dispersion is composed of three branches with only two of them of lower energies being essentially infrared active. Therefore, whatever the importance of NP effects in orbital and spin levels, one should observe, in the Faraday configuration, *at most only* two lines resulting from the mixing of the three one-electron transitions. Because of this mixing, the oscillator strengths of the transitions are significantly modified with respect to those deduced from the one-electron model. The third MP transition which is practically infrared inactive is shifted to higher energies by an amount which depends on the exchange interactions between different LL. Though not directly measurable, these interactions manifest themselves in the magnetic field variation of the CR energies which develops "kinks" at odd integer values of the filling factor  $\nu = n_S \phi_0 / B$  ( $\phi_0$  being the flux quantum and  $n_S$  the areal density of carriers) for  $\nu > 2$ .

### II. EXPERIMENTAL DETAILS

Refined experiments have been performed on single doped GaAs quantum wells (QW) already used in a previous paper.<sup>10</sup> The GaAs QW is sandwiched between two GaAs/AlAs superlattices with the Si-*n*-type doping performed symmetrically on both sides of the QW.<sup>11</sup> The whole epitaxial structure has been lifted off from the growth substrate and deposited on an insulating Si wedged substrate which is

transparent in the far infrared range of energy to avoid the strong optical phonon absorption (reststrahlen band) which occurs in traditional GaAs thick substrates. We have performed magnetoinfrared transmission measurements in the Faraday configuration with unpolarized infrared light using a Bruker Fourier Transform Spectrometer IFS-113 which was connected to a resistive 28 T magnet via a metallic waveguide. All measurements were made at a fixed temperature of 1.8 K. We use a rotating sample holder which allows us to switch *in situ* between the sample and a reference sample. For each value of the magnetic field, we have measured the transmission of the sample and of a reference (a silicon substrate) to normalize the transmission. These measurements are thus absolute measurements and exact absorption amplitudes can be extracted for the comparison with models. Moreover, as optical phonons in the AlAs/GaAs short period superlattice and in the GaAs QW also present infrared signatures we were led to normalize the absolute transmission at a given magnetic field  $B$  by the absolute transmission measured at  $B=0$  T. In the following, these absolute spectra normalized to the  $B=0$  T spectra will be referred to as relative transmission spectra and will then be compared to a simulation<sup>12</sup> of the multilayer transmission taking into account all the different dielectric layers of the sample. The whole procedure minimizes the errors due to experimental or/and dielectric artifacts.

In this paper, we will present results obtained for three samples labeled 1038, 1201, and 1211. The sample 1038 corresponds to a QW width  $L=10$  nm, a carrier density  $n_S=12.8 \times 10^{11} \text{ cm}^{-2}$ , and a mobility of  $\mu_{dc}=114 \text{ m}^2 \text{ V}^{-1} \text{ s}^{-1}$ , whereas for the samples 1201 and 1211, originating from the same wafer,  $L=13$  nm,  $n_S=9.4 \times 10^{11} \text{ cm}^{-2}$ , and  $\mu_{dc}=280 \text{ m}^2 \text{ V}^{-1} \text{ s}^{-1}$ . These concentration and mobility values are obtained from transport measurements performed on parent samples without the lift-off process. The lateral size of the lift-off samples ranges from 3 to 4 mm.

### III. RESULTS

In order to fit the measured infrared transmission, one has to use the components of the dielectric tensor  $\bar{\epsilon}$  of the doped QW. As shown in Ref. 9, these components can be formally written as

$$\begin{aligned} \epsilon_{\parallel} &= \epsilon_L - \frac{(\omega_p)^2}{\omega} \sum_p \frac{I_p(\omega + i\delta_p)}{(\omega + i\delta_p)^2 - (E_p^{\text{MP}})^2}, \\ \epsilon_{\perp} &= -1 - \frac{(\omega_p)^2}{\omega} \sum_p \frac{I_p E_p^{\text{MP}}}{(\omega + i\delta_p)^2 - (E_p^{\text{MP}})^2}, \end{aligned} \quad (1)$$

where  $\epsilon_L$  is the lattice contribution to the diagonal part of the tensor and  $(\omega_p)^2=4\pi n_S e^2 / (Lm^*)$  is the square of the plasma frequency defined for a mean value of the carrier effective mass  $m^*$ . One can note that formally Eq. (1) is very similar to the standard expression derived from the Drude model. However, here the significance of the parameters is different: The summation over  $p(=0,1)$  corresponds to the two CR active MP modes with an energy  $E_p^{\text{MP}}$ , and a corresponding oscilla-

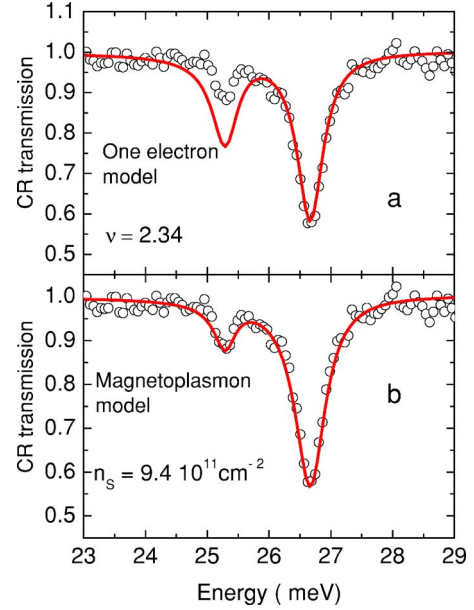


FIG. 1. (Color online) Comparison of CR experimental transmission spectra (open circles) and theoretical simulated spectra (full lines) of sample 1211 for  $\nu=2.34$ . In panel (a) the fit is made using the oscillator strength given by the one-electron model, whereas in panel (b) the oscillator strength of the transitions is fitted (see text).

tor strength  $I_p$ . Both oscillator strengths depend on  $K_{\parallel}=|\vec{K}|$  but are used in the fitting procedure as additional parameters with the constraint that  $\sum_p I_p=1$ . The  $K_{\parallel}$  dependence of  $I_p$  is relatively weak but its value at  $K_{\parallel} \approx 0$  is significantly different from the value obtained in the one-electron model due to the mixing of the one-electron transitions implied in the MP approach.<sup>9</sup> In addition, the damping parameter  $\delta_p$  is used to fit the width of each transition.

To illustrate this point, we compare in Fig. 1 the experimental spectrum for sample 1211 measured at  $\nu=2.34$ , with the simulated spectra using Eq. (1) for two distinct approaches: In Fig. 1(a) the simulation, assuming that the oscillator strength is given by the one-electron model, uses four independent fitting parameters (the energies  $E_0^{\text{MP}}$ ,  $E_1^{\text{MP}}$ , and the respective damping parameters  $\delta_0$ ,  $\delta_1$ ); in Fig. 1(b) an additional fitting parameter ( $I_0$ ) is used to simulate the spectrum. It is clear from the results that using the one-electron model to deduce the carrier concentration of a 2DEG is not correct and, in the present case, leads to a concentration which is 6–8 % lower than the one deduced from transport measurements. This result is of particular importance when interpreting CR data.

Figure 2 and Fig. 3 display the results of the fitting procedure obtained for samples 1201/1211 and 1038, respectively. In the upper panels the data relative to the damping parameters  $\delta_0$  and  $\delta_1$  are reported. On physical grounds, besides a weak constant value of these parameters reflecting the small residual imperfections of the sample, any deviation from this value reflects the presence of an additional dissipative interaction. In order to have a more detailed vision of the variations of energies with the filling factor, the quantities displayed in the lower panel of Fig. 2 and Fig. 3 are  $E_0^{\text{MP}}/B$  (open circles) and  $E_1^{\text{MP}}/B$  (crosses). In the Faraday configu-

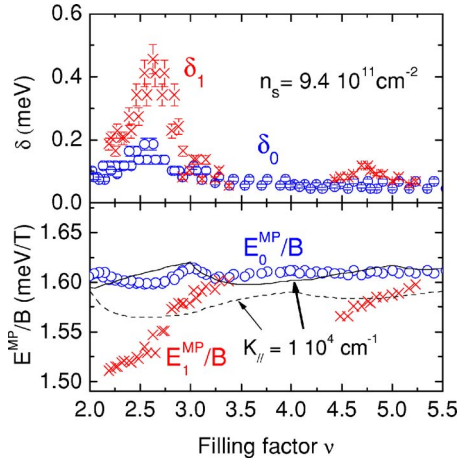


FIG. 2. (Color online) Collected data for samples 1201/1211. Top panel: Variation as a function of  $\nu$  of the fitted damping parameters  $\delta_0$  (open circles) and  $\delta_1$  (crosses) of the CR transitions. Bottom panel: Comparison between the experimental results for  $E_0^{\text{MP}}/B$  (open circles) and  $E_1^{\text{MP}}/B$  (crosses) with the predictions of the MP model for  $K_{\parallel}=1 \times 10^4 \text{ cm}^{-1}$ : Full line corresponds to  $E_0^{\text{MP}}/B$  and dashed line to  $E_1^{\text{MP}}/B$ .

ration, the wave vector of the light  $\vec{q}$  is parallel to  $\vec{B}$  and the only nonzero theoretical component of  $\vec{q}$  is  $q_z$ . Therefore, in principle,  $K_{\parallel}$  should be 0. In practice however one has to face the divergence of the beam which can be important especially when using light pipes to transfer the electromagnetic field. When the full multidielctric treatment is performed<sup>12</sup> to evaluate the transmission of such samples, values for  $q_z=4\pi \text{Re}(\tilde{n})/\lambda$  (where  $\tilde{n}$  is the complex value of the index of refraction and  $\lambda$  is the wavelength corresponding to the CR transition) are found to range between 4 and  $7 \times 10^4 \text{ cm}^{-1}$ . As a consequence, allowing for divergence of the infrared beam leads us to consider values of  $q_{\parallel}=K_{\parallel}$

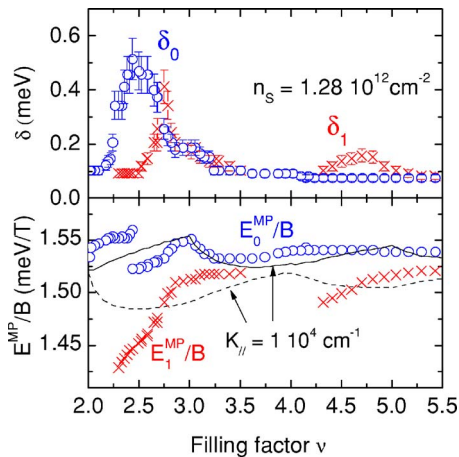


FIG. 3. (Color online) Sample 1038. Top panel: Variation as a function of  $\nu$  of the experimental damping parameter  $\delta_0$  (open circles) and  $\delta_1$  (crosses) of the CR transitions. Bottom panel: Comparison between the experimental results for  $E_0^{\text{MP}}/B$  (open circles) and  $E_1^{\text{MP}}/B$  (crosses) with the predictions of the MP model for  $K_{\parallel}=1 \times 10^4 \text{ cm}^{-1}$ : Full line corresponds to  $E_0^{\text{MP}}/B$  and dashed line to  $E_1^{\text{MP}}/B$ .

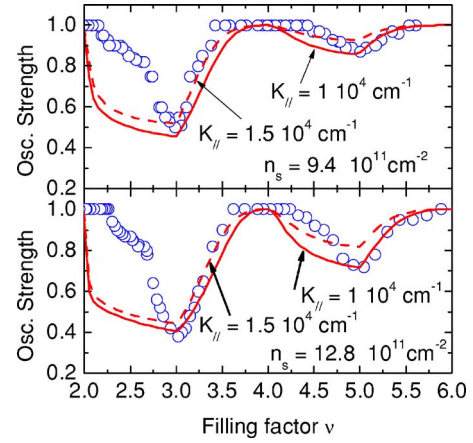


FIG. 4. (Color online) Variation as a function of  $\nu$  of the fitted oscillator strength  $I_0$  of the  $E_0^{\text{MP}}$  transition (open circles) for samples 1201/1211 (top panel) and sample 1038 (bottom panel). These variations are compared to the predictions of the MP model for  $K_{\parallel}=1 \times 10^4 \text{ cm}^{-1}$  (full lines) and  $=1.5 \times 10^4 \text{ cm}^{-1}$  (dashed lines).

$\approx 10^4 \text{ cm}^{-1}$ . We display in the lower panels of Fig. 2 and Fig. 3 the evolutions for both transitions expected from the MP model<sup>9</sup> for  $K_{\parallel}=1 \times 10^4 \text{ cm}^{-1}$  (full and dashed lines). Of course these values vary with the magnetic field and the curves displayed in these figures have to be understood as a frame surrounding the corresponding variations.

As already reported,<sup>9,12</sup> one has to use an independent model to reproduce NP effects in the MP approach and the one used here is that given in Ref. 13 with a fitting parameter, the QW effective gap, adjusted to fit the data for  $E_0^{\text{MP}}/B$  at  $\nu=3$ . Changing this parameter does not modify the shape of the magnetic field evolution of the  $E_p^{\text{MP}}/B$  and only results in a rigid shift.<sup>14</sup> One notes that, for both samples, the variations of  $E_0^{\text{MP}}/B$  as a function of  $\nu$  display a kink at  $\nu=3$  which is well reproduced by the MP model. The discontinuity of  $E_0^{\text{MP}}/B$  observed for the sample 1038 (Fig. 3) at  $\nu \approx 2.4$  occurs, within the experimental error, for  $E_0^{\text{MP}}$  equals the energy  $\hbar\omega_{\text{TO}}$  of the TO phonon mode of GaAs. This discontinuity and the related increase of  $\delta_0$ , also observed in samples 1201/1211 but at  $\nu < 2$ , reflects an interaction previously reported for a doped GaAs QW (Ref. 10), as well as for a doped GaInAs QW.<sup>15</sup> This interaction which apparently concerns  $E_0^{\text{MP}}$  and not  $E_1^{\text{MP}}$  is, at present, not well understood and will not be discussed here. One notes that the variation of  $\delta_0$  is quite smooth as long as  $E_0^{\text{MP}}$  is well below  $\hbar\omega_{\text{TO}}$ . On the other hand, the variation of  $\delta_1$  goes through a pronounced maximum at  $\nu \approx 2.5$  and 4.5. This reflects, as already pointed out, the presence of an additional dissipative interaction mechanism which mainly concerns  $E_1^{\text{MP}}$ .

To complete the report on the fitting procedure, the oscillator strength  $I_0$  of the  $E_0^{\text{MP}}$  transition is displayed in Fig. 4 as a function of  $\nu$  for all samples. The corresponding oscillator strength for  $E_1^{\text{MP}}$  is the complement to 1 of this variation. The fitted oscillator strength goes through a minimum at  $\nu=3$  and 5: The relative depth of these minima depends on  $\nu$  for each sample and also on the carrier concentration. Here the data are compared to the predictions of the MP model for different values of  $K_{\parallel}$ . For any small nonzero value of  $K_{\parallel}$ ,  $I_0$  rises to 1 for  $\nu$  values close to an even integer.

In the following, we will discuss the experimental results obtained in the framework of the MP picture and they will be compared to the expectations of the one-electron picture. First, the evolution of  $E_0^{\text{MP}}/B$  is quite constant for  $2 < \nu < 6$  which is not predicted by the one electron model including NP effects but well reproduced by the MP model. Second, the kink observed clearly for  $\nu=3$  is also well reproduced. This is a fundamental point because, as shown in Ref. 9, the presence of this “kink” is due to the change of the exchange energies across odd filling factors larger than 2 and is a direct signature of the MP effects. A good agreement is also observed for  $I_0$  as far as the minima at odd integer filling factors are concerned as well as their relative variations on  $\nu$  and  $n_s$ . This is in contrast to the predictions of the one-electron model in which not only minima of  $I_0$  do not occur at odd integer values of  $\nu$  but are also independent on  $\nu$  and  $n_s$ . One notes in addition that the results discussed in Fig. 1 become coherent in the MP picture, because the use of carrier densities deduced from the one-electron model would lead to the kink of  $E_0^{\text{MP}}/B$  occurring at filling factors around 2.8 where no physical arguments could justify such a discontinuity. Therefore, it is clear from these data that the MP picture should be considered when interpreting CR experiments. It is important to note here that, whereas the “kink” feature appearing in the energy variation of the  $E_0^{\text{MP}}/B$  has an amplitude decreasing when  $n_s$  decreases, the characteristic extrema of the oscillator strengths at odd filling factors is a robust signature of the MP character of the CR transitions which, in practice, does not depend on the carrier concentration.

There are however apparent discrepancies between the reported data and the predictions of the MP model. First the evolution of  $E_1^{\text{MP}}$  (Fig. 2 and Fig. 3) is not reproduced by the model, especially for  $\nu$  values between 2 and 3, and to a lesser extent between 4 and 5. In the same range of filling factors, the variation of the oscillator strength (Fig. 4) is also not correctly taken into account (because of the sum rule  $\sum_p I_p = 1$ , the discrepancy for  $I_0$  is the consequence of an overestimation of  $I_1$  by the MP model). Further refinements of the MP model, such as changing the NP model<sup>16,17</sup> or introducing spin-orbit interaction,<sup>18</sup> were unable to explain the observed discrepancies.

One can note however that these discrepancies occur when the dissipative mechanism is switched on. Whatever its origin, the occurrence of such a mechanism will lead to a self-energy  $\Sigma(\omega) = \text{Re}(\Sigma(\omega)) + i \text{Im}(\Sigma(\omega))$  which will modify the poles of  $\bar{\epsilon}$ . In the frame of the response theory,  $\text{Im}(\Sigma(\omega))$

and  $\text{Re}(\Sigma(\omega))$  are related to each other by the Kramers-Krönig (KK) relations. Assuming that  $\text{Im}(\Sigma(\omega))$  is reflected by the observed increase of  $\delta_1$  which could be fitted with a Lorentzian curve, the corresponding KK transform develops an “S” shape variation around the maximum of the Lorentzian curve and can explain quantitatively the discrepancies between the experimental and calculated values of  $E_1^{\text{MP}}/B$  in the range of corresponding filling factors. This argument, however has to be considered as an empirical approach to this problem: It does explain, *a priori*, the discrepancies observed for the oscillator strength.

The presence of the dissipative interaction has to be introduced into the MP model in a self-consistent way. To explain the origin of this interaction, it is natural to invoke the effects of impurities which in the present case of high mobility samples should essentially contribute to long range interactions. The theoretical approach of the MP model including these effects is difficult and has only been treated, formally, in the case of integer filling factors<sup>2</sup> where, in the present experimental investigation, nothing spectacular occurs. This approach reveals however that the introduction of such effects leads to an additional modification of the mixing of the wave functions: We therefore believe that a complete treatment of the MP model, introducing impurity interactions, should reproduce self-consistently the observed variation of  $E_1^{\text{MP}}/B$  and explain the discrepancies observed in the oscillator strengths.

#### IV. CONCLUSION

In conclusion, careful far infrared magnetotransmission measurements performed on a series of doped GaAs QW reveal many specific features in the evolution of the CR energies and of their oscillator strengths which can be understood in the frame of the MP picture developed without any additional dissipative interaction. This proves that cyclotron resonance excitations in semiconductors are indeed magnetoplasmon excitations due to many-body interactions, which have to be taken into account when analyzing cyclotron resonance experiments.

#### ACKNOWLEDGMENTS

The GHMFL is “Laboratoire conventionné l’UJF et l’INPG de Grenoble.” The work presented here has been supported in part by the European Commission through Grant No. RITA-CT-2003-505474.

<sup>1</sup>Yu. A. Bychkov, S. V. Iordanskii, and G. M. Eliashberg, Pis’ma Zh. Eksp. Teor. Fiz. Pis’ma Zh. Eksp. Teor. Fiz. **33**, 152 (1981); [JETP Lett. **33**, 143 (1981)].

<sup>2</sup>C. Kallin and B. I. Halperin, Phys. Rev. B **31**, 3635 (1985).

<sup>3</sup>A. H. MacDonald and C. Kallin, Phys. Rev. B **40**, 5795 (1989).

<sup>4</sup>Yu. A. Bychkov and G. Martinez, Phys. Rev. B **66**, 193312 (2002).

<sup>5</sup>W. Kohn, Phys. Rev. **123**, 1242 (1961).

<sup>6</sup>K. Ensslin, D. Heitmann, H. Sigg, and K. Ploog, Phys. Rev. B **36**,

8177 (1987).

<sup>7</sup>C. M. Hu, E. Batke, K. Kohler, and P. Ganser, Phys. Rev. Lett. **75**, 918 (1995).

<sup>8</sup>M. Manger, E. Batke, R. Hey, K. J. Friedland, K. Kohler, and P. Ganser, Phys. Rev. B **63**, 121203(R) (2001).

<sup>9</sup>Yu. A. Bychkov and G. Martinez, Phys. Rev. B **72**, 195328 (2005).

<sup>10</sup>C. Faugeras, G. Martinez, A. Riedel, R. Hey, K. J. Friedland, and Yu. Bychkov, Phys. Rev. Lett. **92**, 107403 (2004).

- <sup>11</sup>K. J. Friedland, R. Hey, H. Kostial, R. Klann, and K. Ploog, *Phys. Rev. Lett.* **77**, 4616 (1996).
- <sup>12</sup>Yu. Bychkov, C. Faugeras, and G. Martinez, *Phys. Rev. B* **70**, 085306 (2004).
- <sup>13</sup>C. Hermann and C. Weisbuch, *Phys. Rev. B* **15**, 823 (1977).
- <sup>14</sup>We adjust this parameter at  $\nu=3$  in order to compare the theoretical and experimental shapes of the “kink.”
- <sup>15</sup>C. Faugeras, G. Martinez, F. Capotondi, G. Biasol, and L. Sorba, *Europhys. Lett.* **67**, 1031 (2004).
- <sup>16</sup>U. Ekenberg, *Phys. Rev. B* **40**, 7714 (1989).
- <sup>17</sup>V. G. Golubev, V. I. Ivanov-Omskii, I. G. Minervin, A. V. Osutin, and D. G. Polyakov, *Zh. Eksp. Teor. Fiz.* **88**, 2052 (1985); [*Sov. Phys. JETP* **61**, 1214 (1985)].
- <sup>18</sup>Y. A. Bychkov and E. I. Rashba, *J. Phys. C* **17**, 6039 (1984).